Performance Analysis of Slow Fluid Antenna Multiple Access in Noisy Channels using Gauss-Laguerre and Gauss-Hermite Quadratures

Halvin Yang, *Student Member, IEEE,* Kai-Kit Wong, *Fellow, IEEE,* Kin-Fai Tong, *Fellow, IEEE,* Yangyang Zhang, and Chan-Byoung Chae, *Fellow, IEEE*

***Abstract*—Fluid antenna system (FAS) facilitating a position-switchable antenna, enables a mobile receiver to exploit the deep fade opportunity of its interference for multiple access. Slow fluid antenna multiple access (s-FAMA) is such an emerging proposal that lets multiple users share the same time-frequency channel while each user adopts a fluid antenna to resolve the interference. Previous performance analysis is limited to the case when noise is neglected. In this letter, we remove this limitation and derive new closed-form expressions for the outage probability of s-FAMA by using Gauss-Laguerre and Gauss-Hermite Quadratures. The analysis reveals the impact of noise on the outage probability for different numbers of users and ports in s-FAMA networks.**

***Index Terms*—Fluid antenna, Gaussian approximation, Gauss-Laguerre quadrature, Multiple Access, Outage probability.**

I. Introduction

MULTIPLE access is the backbone of mobile communications, which aims to allocate the spectrum to multiple mobile users in the most efficient manner for communications. With the ever-increasing demand on massive connectivity in the fifth generation (5G) and beyond, it is strongly desirable to have a multiple access technology that can accommodate a large number of users on a single channel. Conventionally, this is largely achieved by using multiuser multiple-input multiple-output (MIMO) precoding [1]. Non-orthogonal multiple access (NOMA) is another technology that is widely tipped to shine in conjunction with MIMO for greater capacity [2]. While the merits of MIMO and NOMA are recognized, their complexities are constantly questioned. To name just a few, the channel state information (CSI) acquisition for the base station (BS), the complex optimization for MIMO precoding matrices and power allocation, and for NOMA the interference cancellers, are some of the obstacles that hinder their scalability.

Recently, a new multiple access technique, which is referred to as fluid antenna multiple access (FAMA), emerges [3]. This scheme employs a fluid antenna system (FAS) at each mobile user which is equipped with the ability to access the null of its interference, created naturally by fading, for multiple access. FAS uses either a liquid-based antenna [4] or reconfigurable pixel-based antenna [5], [6] that facilitates mobilization of the radiating element to access fading at different locations. Before reviewing the latest FAMA work, it is worth mentioning that research in single-user FAS only began a few years ago and it was first introduced by Wong *et al.* in [7]. Since then, [8] looked to improve the channel correlation model for a more accurate performance analysis of FAS while [9] attempted to design coded modulation schemes for a FAS. The performance of FAS in Nakagami fading channels was also studied in [10]. Later, [11] tackled the CSI estimation problem for FAS.

However, FAMA utilizing FAS at each mobile user is much less understood. It has two types: fast FAMA (f-FAMA) [12], [13] and slow FAMA (s-FAMA) [14], [15]. In f-FAMA, the fluid antenna at each user is switched to the location (referred to as 'port') that achieves the maximum instantaneous channel energy to the energy of the sum-interference plus noise ratio on a symbol-by-symbol basis. By contrast, s-FAMA represents a practical alternative where each user switches its fluid antenna port only if the channel changes. Unlike multiuser MIMO and NOMA, both FAMA approaches do not require CSI at the BS, no complex optimization for precoding and power allocation, nor multiuser detector at the mobile user. Interference in the FAMA network is dealt with entirely by each user activating its antenna port where its interference naturally vanishes due to fading. It was found in [12], [14] that with enough resolution and size of the fluid antenna, FAMA could support a massive number of users on a single time-frequency channel.

Though [14] presented the outage probability analysis, noise was excluded. Noting that 5G is heading to a ultra low-power regime [16], the high signal-to-noise ratio (SNR) assumption is increasingly doubtful. Motivated by this, this letter revisits the performance analysis of the s-FAMA network by considering the presence of noise.[1] For mathematical tractability, we adopt Gaussian approximation to model the distribution of the sum of interference and noise power at each fluid antenna port, and then derive a closed-form expression for the outage probability using Gauss-Laguerre and Gauss-Hermite quadratures.

II. System Model

We consider a downlink system where a BS with U fixed antennas is communicating to U mobile users each equipped with an N-port fluid antenna of size $W\lambda$ in which λ denotes the wavelength and W denotes the normalized size of the fluid antenna. For simplicity, we assume that each fluid antenna has

The work of Wong and Tong is supported by the Engineering and Physical Sciences Research Council (EPSRC) under Grant EP/W026813/1. For the purpose of open access, the authors will apply a Creative Commons Attribution (CC BY) licence to any Author Accepted Manuscript version arising.

The work of C. B. Chae is supported by the Institute for Information and Communication Technology Promotion (IITP) grant funded by the Ministry of Science and ICT (MSIT), Korea (No. 2021-0-02208, No. 2021-0-00486).

H. Yang, K. K. Wong and K. F. Tong are with the Department of Electronic and Electrical Engineering, University College London, WC1E 7JE, United Kingdom. *Corresponding author:* kai-kit.wong@ucl.ac.uk.

Y. Zhang is with Kuang-Chi Science Limited, Hong Kong SAR, China.

K. K. Wong and C. B. Chae are with Yonsei Frontier Lab, School of Integrated Technology, Yonsei University, Seoul, 03722, Korea.

[1]The objective of this work is to improve the outage performance analysis of s-FAMA with noise. Therefore, we will not attempt to compare s-FAMA with other multiple access schemes. It is also not meaningful to use outage probability for performance comparison between different multiple access schemes as they treat interference differently. For example, with CSI at the BS, multiuser MIMO ensures no interference at the users while NOMA subtracts interference iteratively at the users. By contrast, s-FAMA is a much simpler approach, does not need CSI at the BS and treats interference as noise.

a line shape and takes up only a one-dimensional space. The U antennas at the BS are assumed to be situated far apart so that their channels are independent. Each of the BS antennas is dedicated to transmit to one mobile user. All communications takes place on the same time-frequency channel. For the u-th mobile user, each port represents a physical location at which the signal can be received. At the k-th port, we have

$$r_k^{(u)} = g_k^{(u,u)} s_u + \sum_{\substack{\tilde{u}=1 \\ \tilde{u}\neq u}}^{U} g_k^{(\tilde{u},u)} s_{\tilde{u}} + \eta_k^{(u)}, \tag{1}$$

where s_u represents the transmitted symbol for the u-th user, $g_k^{(\tilde{u},u)}$ is the complex channel from the $\tilde{u}$-th BS antenna to the k-th port of the fluid antenna at the u-th user, and $\eta_k^{(u)}$ is the complex additive white Gaussian noise (AWGN) at the k-th port of the u-th user with zero mean and variance of σ_η^2. The average symbol energy is assumed to be $\mathrm{E}[|s_u|^2] = \sigma_s^2$.

As W is finite but N can be very large, the channels at the ports, $\{g_k^{(\tilde{u},u)}\}_{\forall k}$, are correlated. To model this, the channel is parametrized via the correlation parameter μ as [17]

$$\begin{aligned} g_k^{(\tilde{u},u)} = \sigma_g(\sqrt{1-\mu^2} x_k^{(\tilde{u},u)} + \mu x_0^{(\tilde{u},u)}) \\ + j\sigma_g(\sqrt{1-\mu^2} y_k^{(\tilde{u},u)} + \mu y_0^{(\tilde{u},u)}), \end{aligned} \tag{2}$$

where $x_0, \ldots, x_K, y_0, \ldots, y_K$ are all independent and identically distributed (i.i.d.) Gaussian random variables each with zero mean and a variance of 0.5. With a linear size of $W\lambda$, the correlation parameter, μ, can be set by

$$\mu = \sqrt{2}\sqrt{{}_1F_2\left(\frac{1}{2}; 1, \frac{3}{2}; -\pi^2 W^2\right) - \frac{J_1(2\pi W)}{2\pi W}}, \tag{3}$$

in which ${}_1F_2$ is the generalized hypergeometric function and $J_1(\cdot)$ is the first-order Bessel function of the first kind [17]. Instead of this model (2), it is also possible to use the finite-scatterer model which is popularly applied for millimeter-wave channels [18]. However, it was found in [14] that both models will generate similar results especially when the target signal-to-interference plus noise ratio (SINR) is not too large; yet the model (2) is preferred for its mathematical tractability.

In this letter, s-FAMA is considered. Hence, user u chooses the antenna port that maximizes the SINR, i.e.,[2]

$$k^* = \arg\max_k \mathrm{SINR}_k^{(u)} \tag{4a}$$

$$= \arg\max_k \frac{\sigma_s^2 |g_k^{(u,u)}|^2}{\sigma_s^2 \sum_{\substack{\tilde{u}=1 \\ \tilde{u}\neq u}}^{U} |g_k^{(\tilde{u},u)}|^2 + \sigma_\eta^2} \equiv \arg\max_k \frac{X_k^{(u)}}{Y_k^{(u)}}. \tag{4b}$$

The performance of the s-FAMA network can be characterized by the outage probability

$$p = \mathrm{E}\left[\mathrm{Prob}\left(\mathrm{SINR}_{k^*}^{(u)} < \gamma\right)\right] \overset{(a)}{=} \mathrm{Prob}\left(\mathrm{SINR}_{k^*} < \gamma\right), \tag{5}$$

where (a) is obtained by dropping the user index because the users are assumed i.i.d., and γ is the SINR threshold.

[2]If $\sigma_\eta = 0$ in (4b), then the outage probability analysis is proved possible in the form of the integral of the generalized Marcum-Q function [14, (21)]. However, in this work, $\sigma_\eta \neq 0$ and the analysis in [14] is no longer possible.

III. New Outage Probability Expressions

Before we proceed to present our main results, it is worth pointing out that [14] attempted to derive the outage probability (5). However, this was only achieved if σ_η^2 in (4) was set to 0 so that the denominator of the SINR, Y_k, was noncentral Chi-square distributed and the outage probability involving the integral could be evaluated. With $\sigma_\eta^2 \neq 0$, this is no longer true. To overcome this, we resort to Gaussian approximation [19] to model the distribution of Y_k which would be accurate when U is large. In this section, our objective is to evaluate:

$$\begin{aligned} p &= \mathrm{Prob}(\mathrm{SINR}_{k^*} < \gamma) \\ &= \mathrm{Prob}(X_1 < \gamma Y_1, X_2 < \gamma Y_2, \ldots, X_N < \gamma Y_N), \end{aligned} \tag{6}$$

which can further be evaluated as

$$\begin{aligned} p = \int \cdots \int & F_{X_1,\ldots,X_N|Y_1,\ldots,Y_N}(\gamma y_1, \ldots, \gamma y_N) \\ & \times f_{Y_1,Y_2,\ldots,Y_N}(y_1, y_2, \ldots, y_N) dy_1 dy_2 \cdots dy_N, \end{aligned} \tag{7}$$

where $f_{Y_1,\ldots,Y_N}(\cdots)$ is the joint probability density function (PDF) of $Y_1, \ldots, Y_N$ and $F_{X_1,\ldots,X_N|Y_1,\ldots,Y_N}(\cdots)$ represents the cumulative density function (CDF) of $X_1, \ldots, X_N$ conditioned on the random variables $Y_1, Y_2, \ldots, Y_N$.

Lemma 1: The conditional CDF in (6) can be obtained as

$$\begin{aligned} & F_{X_1,\ldots,X_N|Y_1,\ldots,Y_N}(\gamma y_1, \ldots, \gamma y_N) = \\ & \frac{1}{2}\int_0^\infty e^{-\frac{\tilde{r}}{2}} \prod_{k=1}^{N} \left[1 - Q_1\left(\sqrt{\frac{\mu^2}{1-\mu^2}}\tilde{r}, \sqrt{\gamma y_k}\right)\right] d\tilde{r}, \end{aligned} \tag{8}$$

where $Q_1(a, b)$ is the first-order Marcum Q-function.

Proof: The conditional CDF can be readily obtained using [14, (60)] by substituting $t_1 = \gamma y_1, \ldots, t_N = \gamma y_N$. ■

Theorem 1: The joint PDF of $Y_1, \ldots, Y_N$ for the s-FAMA system can be approximated by

$$\begin{aligned} & f_{Y_1,Y_2,\ldots,Y_N}(y_1, y_2, \ldots, y_N) \approx \\ & \int_{-\infty}^{\infty} \frac{e^{-\frac{r^2}{2\sigma_y^2}}}{\sqrt{2\pi}\sigma_y} \prod_{k=1}^{N} \frac{1}{\sqrt{2\pi(1-\lambda_y^2)}\sigma_y} e^{-\frac{(y_k - \lambda_y r - \mu_y)^2}{2(1-\lambda_y^2)\sigma_y^2}} dr, \end{aligned} \tag{9}$$

where

$$\begin{cases} \mu_y = \sigma_s^2 \sigma_g^2 (U-1) + \sigma_\eta^2, \\ \sigma_y = \sigma_s^2 \sigma_g^2 \sqrt{U-1}, \\ \lambda_y = \dfrac{\mu}{1 + 2\mu^2 - 2\mu^4}. \end{cases} \tag{10}$$

Proof: See Appendix A. ■

While the use of Gaussian approximation may be seen as a straightforward approach that greatly simplifies the derivation of the joint PDF, the overall approach is not trivial because of the introduction of λ_y that reinstates the correlation amongst the random variables $Y_1, Y_2, \ldots, Y_N$.

Theorem 2: The outage probability of the s-FAMA system, p, is given by (11) (see top of next page).

Proof: Substituting (9) and (8) into (7) and after some simplification, (11) is obtained, which completes the proof. ■

In the next theorem, we present a new closed-form expression for the outage probability of s-FAMA where both noise

$$p = \frac{1}{2\sqrt{2\pi}\sigma_y}\int_0^\infty e^{-\frac{\tilde{r}^2}{2}}\int_0^\infty e^{-\frac{r^2}{2\sigma_y^2}}\prod_{k=1}^{N}\left[1-\frac{1}{\sqrt{2\pi(1-\lambda_y^2)\sigma_y}}\int_{y_k=0}^\infty Q_1\left(\sqrt{\frac{\mu^2}{1-\mu^2}}\tilde{r},\sqrt{\gamma y_k}\right)e^{-\frac{(y_k-\lambda_y r-\mu_y)^2}{2(1-\lambda_y^2)\sigma_y^2}}dy_k\right]dr d\tilde{r} \tag{11}$$

and interference are present. The result uses Gauss-Laguerre and Gauss-Hermite quadratures in the following lemmas.

Lemma 2: The Gauss-Laguerre quadrature is given by [20, p. 923]

$$\int_0^\infty g(x)dx \approx \sum_{i=1}^{n} w_i e^{\alpha_i} g(\alpha_i), \tag{12}$$

where α_i is the i-th root of Laguerre polynomial $L_n(x)$, and

$$w_i = \frac{\alpha_i}{(n+1)^2\left(L_{n+1}(\alpha_i)\right)^2}. \tag{13}$$

Lemma 3: The Gauss-Hermite quadrature is given by [20, p. 924]

$$\int_{-\infty}^\infty g(x)dx \approx \sum_{i=1}^{n} v_i e^{\beta_i^2} g(\beta_i), \tag{14}$$

where β_i is the i-th root of Hermite polynomial $H_n(x)$, and

$$v_i = \frac{2^{n-1}n!\sqrt{\pi}}{n^2\left(H_{n-1}(\beta_i)\right)^2}. \tag{15}$$

Theorem 3: The outage probability of the s-FAMA system, p, can be approximated in closed form as (16) (see next page) in which w_i and v_j are defined, respectively, in (13) and (15), and also α_i and β_i are, respectively, the i-th root of Laguerre polynomial $L_n(x)$ and Hermite polynomial $H_n(x)$.

Proof: See Appendix B. ∎

The advantage of Theorem 3 is that a closed-form expression can be found, which is not possible otherwise. However, the parameter, n, needs to be selected carefully to result in an accurate approximation. In terms of computational complexity, (16) results in an overall complexity of $O(n^3)$.

IV. Numerical Results

Here, we provide the numerical results to check the accuracy of the proposed expressions, (11) and (16). We do so by including Monte-Carlo simulation results averaging over a large number of independent channel realizations for comparison. In particular, the following results are provided:

- Monte-Carlo—It runs a large of independent simulations and computes the outage probability based on the channel, modelled statistically by (2) and (3).
- Non-closed form (11)—This is the exact expression for the outage probability of a typical s-FAMA user.
- Closed-form (16) with a given n—This is the proposed closed-form analytical expression for approximating the outage probability where the parameter n in (16) controls the level of accuracy as well as complexity. In the figures, we consider the cases $n = 20, 30, 40$.

We will use the numerical results to understand how the s-FAMA network performs in noisy channels under a wide range of system conditions, e.g., varying the average SNR at each user, the SINR threshold for an outage event, γ, the number of users, U, the normalized size of the fluid antenna at each user, W and the number of ports of each fluid antenna, N.

First and foremost, all the results in the figures show that the non-closed form expression (11) is correct, matching the Monte-Carlo simulation results in all the cases. A quick glance of the results further suggests that the proposed closed-form expression (16) is accurate although we will analyze later the impact of n in the accuracy later. Fig. 1 demonstrates how the outage probability changes as the average SNR increases considering $W = 1$ and $\gamma = 10$dB. The results reveal that the outage probability reduces if SNR increases, as expected. Also, the outage probability reduction can be considerable, especially when U is small or N is large, which confirms the importance of analysis considering the presence of noise.

In terms of accuracy for (16), we see that as expected, the accuracy improves if n increases. That said, (16) with $n = 20$ can be sufficiently accurate if the outage probability value is not extremely small such as in the cases $(U, N) = (10, 50)$ and $(U, N) = (10, 100)$. A different phenomenon is, however, observed in the results of Fig. 2 where the outage probability results are plotted against the SINR threshold, γ, assuming the average SNR is 10dB. The results show that (16) is very accurate except when γ becomes very large, say ≥ 20dB.

With the accuracy of (16) confirmed, we now make interesting observations from the results obtained. First, from the results in Fig. 1, it can be observed that as large as $U = 10$ users can be supported with an acceptable outage probability if the number of ports, N, is large enough. Additionally, the systems, $(U, N) = (5, 50)$ and $(U, N) = (10, 500)$, perform very similarly. Hence, supporting more users comes with an increase in the number of ports for resolving the interference. On the other hand, Fig. 2 illustrates that if $\gamma > 10$dB, the outage probability can shoot up quickly if $(U, N) = (10, 50)$ or $(U, N) = (10, 100)$. If N increases or U reduces, the same phenomenon still occurs but it just happens at a larger γ.

Finally, the results of Figs. 3 and 4 investigate the impact of U, N and W on the outage probability performance assuming $\Gamma = \gamma = 10$dB. Apparently, the performance improves if N and/or W increases while the outage probability rises if more users, U, are accommodated. Again, the proposed closed-form expression (16) is accurate in the entire range of settings.

V. Conclusion

In this letter, we revisited the outage probability analysis for the s-FAMA system where the spectral resource was shared aggressively and each user utilized an N-port fluid antenna to resolve the interference. Different from existing studies, noise was considered. To overcome the mathematical challenge, we first utilized Gaussian approximation to work out the joint PDF of the sum-interference plus noise power at all the ports. One major contribution was the derivation of the cross-correlation

$$p \approx \frac{1}{\sqrt{\pi}} \sum_{\ell=1}^{n} w_\ell \sum_{j=1}^{n} v_j \left[1 - \frac{1}{\sqrt{2\pi(1-\lambda_y^2)\sigma_y}} \sum_{i=1}^{n} w_i Q_1 \left(\sqrt{\frac{2\mu^2\alpha_\ell}{1-\mu^2}}, \sqrt{\gamma\alpha_i} \right) e^{\alpha_i - \frac{(\alpha_i - \sqrt{2}\lambda_y \sigma_y \beta_j - \mu_y)^2}{2(1-\lambda_y^2)\sigma_y^2}} \right]^N \tag{16}$$

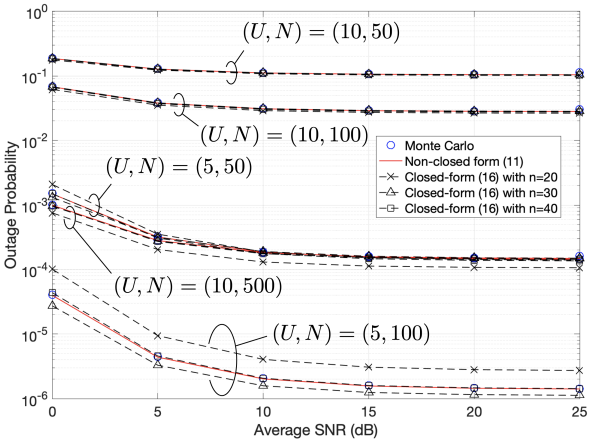

Fig. 1. Outage probability against the average SNR, $\Gamma = \frac{\sigma_g^2 \sigma_s^2}{\sigma_\eta^2}$.

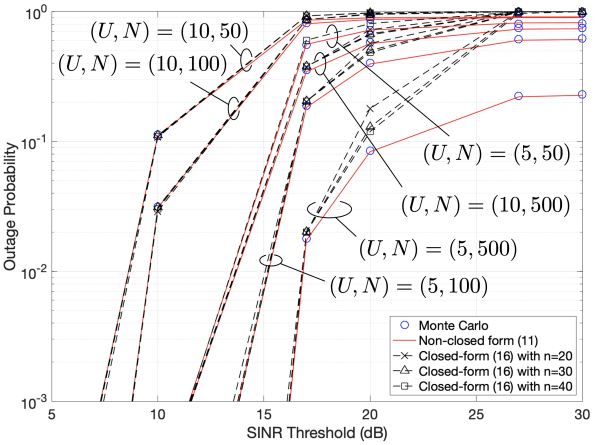

Fig. 2. Outage probability against the SINR threshold, γ.

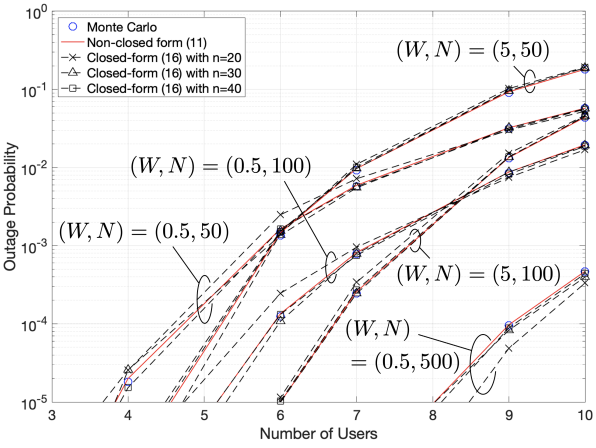

Fig. 3. Outage probability against the number of users, U.

parameter of the joint PDF. Afterwards, we derived the outage probability expression in closed form by using Gauss-Laguerre and Gauss-Hermite quadratures. Our numerical results showed

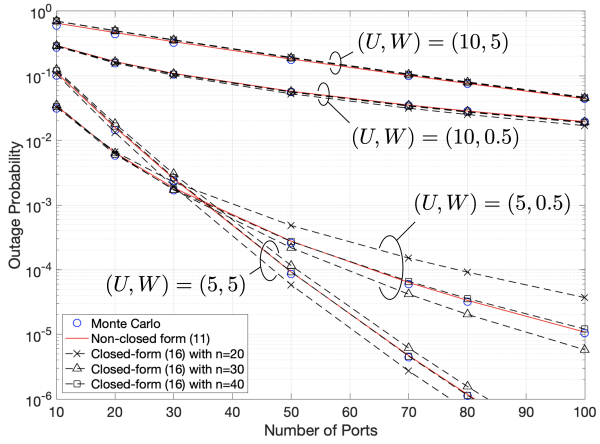

Fig. 4. Outage probability against the number of ports, N.

that the proposed closed-form expression was accurate in the entire range of settings if the SINR threshold, γ, was not too large. The results also revealed the capability of s-FAMA.

APPENDICES

A. Proof of Theorem 1

For large U, the marginal distribution of Y_k is Gaussian, i.e., $Y_k \sim \mathcal{N}(\mu_y, \sigma_y^2)$ with some mean μ_y and variance σ_y^2. The mean μ_y can be found as $\mu_y = \mathrm{E}[\sigma_s^2 \sum_{\tilde{u} \neq u} |g_k^{(\tilde{u},u)}|^2 + \sigma_\eta^2] = \sigma_s^2(U-1)\sigma_g^2 + \sigma_\eta^2$, while the variance σ_y^2 can also be obtained by $\sigma_y^2 = \mathrm{E}[Y_k^2] - \mu_y^2 = \sigma_s^4(U-1)\sigma_g^4$.

Now, we need to construct $\{Y_k\}$ so that they are correlated. To do so, we use a model similar to (2) through a correlation parameter λ_y. That is to say, we have

$$Y_k = \sigma_y(\lambda_y Z_0 + \sqrt{1-\lambda_y^2} Z_k) + \mu_y, \text{ for } k = 1, \ldots, N, \tag{17}$$

where $Z_0, \ldots, Z_N$ are i.i.d. standard Gaussian random variables. With (17), we compute the conditional statistics as

$$\begin{cases} \mathrm{E}[Y_k | \sigma_y Z_0] = \sigma_y \lambda_y Z_0 + \mu_y, \\ \mathrm{Var}[Y_k | \sigma_y Z_0] = (1-\lambda_y^2)\sigma_y^2. \end{cases} \tag{18}$$

Note that conditioned on $\sigma_y Z_0$, all $\{Y_k\}$ will be independent. Therefore, the joint PDF can be obtained by multiplying all the conditional marginal PDFs and then integrating over the PDF of $\sigma_y Z_0$, which gives rise to (9).

The remaining task is to derive λ_y in terms of μ that can capture the correlation structure of $\{Y_k\}$. To do so, we consider the correlation coefficient between Y_k and Y_ℓ given by

$$\rho(Y_k, Y_\ell) = \frac{\mathrm{Cov}(Y_k, Y_\ell)}{\mathrm{Var}(Y_k)\mathrm{Var}(Y_\ell)}. \tag{19}$$

Using (17), it can be easily shown that

$$\rho(Y_k, Y_\ell) = \frac{\lambda_y^2}{\sigma_y^2}. \tag{20}$$

Now, we compute Y_k based on (2) and (4b) which gives

$$Y_k^{(u)} = \sigma_s^2\sigma_g^2\Bigg[\mu^2\sum_{\tilde{u}\neq u}\left(x_0^{(\tilde{u},u)}\right)^2 + 2\mu\sqrt{1-\mu^2}\sum_{\tilde{u}\neq u}x_0^{(\tilde{u},u)}x_k^{(\tilde{u},u)} + (1-\mu^2)\sum_{\tilde{u}\neq u}\left(x_k^{(\tilde{u},u)}\right)^2 + \mu^2\sum_{\tilde{u}\neq u}\left(y_0^{(\tilde{u},u)}\right)^2 + 2\mu\sqrt{1-\mu^2}\sum_{\tilde{u}\neq u}y_0^{(\tilde{u},u)}y_k^{(\tilde{u},u)} + (1-\mu^2)\sum_{\tilde{u}\neq u}\left(y_k^{(\tilde{u},u)}\right)^2\Bigg] + \sigma_\eta^2, \quad (21)$$

where the user index u is reinstated for clarity. Then we get

$$\begin{aligned}\mathrm{Cov}(Y_k, Y_\ell) = \sigma_s^4\sigma_g^4\Big[&\mu^4\mathrm{Cov}\left(\sum x_0^2, \sum x_0^2\right) + 2\mu^3\sqrt{1-\mu^2}\mathrm{Cov}\left(\sum x_0^2, \sum x_0x_\ell\right) + 2\mu^3\sqrt{1-\mu^2}\ \mathrm{Cov}\left(\sum x_0x_k, \sum x_0^2\right) \\ &+ 4\mu^2(1-\mu^2)\mathrm{Cov}\left(\sum x_0x_k, \sum x_0x_\ell\right) + \mu^4\mathrm{Cov}\left(\sum y_0^2, \sum y_0^2\right) \\ &+ 2\mu^3\sqrt{1-\mu^2}\mathrm{Cov}\left(\sum y_0^2, \sum y_0y_\ell\right) + 2\mu^3\sqrt{1-\mu^2}\ \mathrm{Cov}\left(\sum y_0y_k, \sum y_0^2\right) \\ &+4\mu^2(1-\mu^2)\mathrm{Cov}\left(\sum y_0y_k, \sum y_0y_\ell\right)\Big]. \quad (22)\end{aligned}$$

Noting that

$$\begin{cases}\mathrm{Cov}\left(\sum a_0^2, \sum a_0^2\right) = 0.25(U-1), \\ \mathrm{Cov}\left(\sum a_0^2, \sum a_0a_k\right) = 0, \\ \mathrm{Cov}\left(\sum a_0a_k, \sum a_0a_\ell\right) = 0,\end{cases} \quad (23)$$

it can then be derived that

$$\begin{cases}\mathrm{Cov}(Y_k, Y_\ell) = 0.25\sigma_s^4\sigma_g^4\mu^2(U-1), \\ \mathrm{Var}(Y_k) = 0.5\sigma_s^4\sigma_g^4(U-1)\left(1+2\mu^2-2\mu^4\right).\end{cases} \quad (24)$$

Substituting (24) into (19) to obtain $\rho(Y_k, Y_\ell)$ and equating it to (20), we obtain the following condition

$$\frac{\lambda_y^2}{\sigma_y^2} = \frac{0.25\sigma_s^4\sigma_g^4\mu^2(U-1)}{\left[0.5\sigma_s^4\sigma_g^4(U-1)\left(1+2\mu^2-2\mu^4\right)\right]^2}. \quad (25)$$

Finally, substituting the expression of σ_y in (10) into the above and after some simplifications, λ_y in (10) is obtained.

B. Proof of Theorem 3

We begin by expressing the outage probability in (11) as

$$p = \frac{\mathcal{I}_3}{2\sqrt{2\pi}\sigma_y}, \quad (26)$$

where $\mathcal{I}_3 \triangleq \int_0^\infty e^{-\frac{\tilde{r}}{2}}\mathcal{I}_2(\tilde{r})d\tilde{r}$, in which

$$\mathcal{I}_2(z) = \sqrt{2}\sigma_y\int_{-\infty}^{\infty}e^{-t^2}\left[1 - \frac{\mathcal{I}_1\left(z, \sqrt{2}\sigma_y t\right)}{\sqrt{2\pi(1-\lambda_y^2)}\sigma_y}\right]^N dt, \quad (27)$$

where

$$\mathcal{I}_1(z,r) = \int_0^\infty e^{-y}Q_1\left(\sqrt{\frac{\mu^2 z}{1-\mu^2}}, \sqrt{\gamma y}\right)e^{y-\frac{(y-\lambda_y r-\mu_y)^2}{2(1-\lambda_y^2)\sigma_y^2}}dy. \quad (28)$$

After that, we apply Gauss-Laguerre quadrature in Lemma 2 to evaluate (28) and use it in (27). Then we employ Gauss-Hermite quadrature in Lemma 3 to obtain (27) that is substituted back to compute $\mathcal{I}_3$. A closed-form expression for $\mathcal{I}_3$ is then derived using Gauss-Laguerre quadrature again.

REFERENCES

[1] A. Ghosh, A. Maeder, M. Baker and D. Chandramouli, "5G evolution: A view on 5G cellular technology beyond 3GPP Release 15," *IEEE Access*, vol. 7, pp. 127639–127651, Sept. 2019.

[2] L. Zhu, Z. Xiao, X.-G. Xia and D. Oliver Wu, "Millimeter-wave communications with non-orthogonal multiple access for B5G/6G," *IEEE Access*, vol. 7, pp. 116123–116132, Aug. 2019.

[3] K. K. Wong, K. F. Tong, Y. Shen, Y. Chen, and Y. Zhang, "Bruce Lee-inspired fluid antenna system: Six research topics and the potentials for 6G," *Frontiers in Commun. and Netw., section Wireless Commun.*, 3:853416, Mar. 2022.

[4] Y. Huang, L. Xing, C. Song, S. Wang and F. Elhouni, "Liquid antennas: Past, present and future," *IEEE Open J. Antennas and Propag.*, vol. 2, pp. 473–487, Mar. 2021.

[5] A. Grau Besoli and F. De Flaviis, "A multifunctional reconfigurable pixeled antenna using MEMS technology on printed circuit board," *IEEE Trans. Antennas & Propag.*, vol. 59, no. 12, pp. 4413–4424, Dec. 2011.

[6] S. Song and R. D. Murch, "An efficient approach for optimizing frequency reconfigurable pixel antennas using genetic algorithms," *IEEE Trans. Antennas & Propag.*, vol. 62, no. 2, pp. 609–620, Feb. 2014.

[7] K. K. Wong, A. Shojaeifard, K. F. Tong, and Y. Zhang, "Fluid antenna systems," *IEEE Trans. Wireless Commun.*, vol. 20, no. 3, pp. 1950–1962, Mar. 2021.

[8] M. Khammassi, A. Kammoun, and M.-S. Alouini, "A new analytical approximation of the fluid antenna system channel," *IEEE Trans. Wireless Commun.*, 2023.

[9] C. Psomas, G. M. Kraidy, K. K. Wong, and I. Krikidis, "On the diversity and coded modulation design of fluid antenna systems," [Online] arXiv preprint arXiv:2205.01962, 2022.

[10] L. Tlebaldiyeva, G. Nauryzbayev, S. Arzykulov, A. Eltawil, and T. Tsiftsis, "Enhancing QoS through fluid antenna systems over correlated Nakagami-m fading channels," in Proc. *IEEE Wireless Commun. & Netw. Conf. (WCNC)*, pp. 78–83, 10-13 Apr. 2022, Austin, TX, USA.

[11] C. Skouroumounis and I. Krikidis, "Fluid antenna with linear MMSE channel estimation for large-scale cellular networks," *IEEE Trans. Commun.*, vol. 71, no. 2, pp. 1112–1125, Feb. 2023.

[12] K. K. Wong, and K. F. Tong, "Fluid antenna multiple access," *IEEE Trans. Wireless Commun.*, vol. 21, no. 7, pp. 4801–4815, Jul. 2022.

[13] K. K. Wong, K. F. Tong, Y. Chen, and Y. Zhang, "Fast fluid antenna multiple access enabling massive connectivity," *IEEE Commun. Lett.*, vol. 27, no. 2, pp. 711–715, Feb. 2023.

[14] K. K. Wong, D. Morales-Jimenez, K. F. Tong, and C. B. Chae, "Slow fluid antenna multiple access," to appear in *IEEE Trans. Commun.*, 2023.

[15] N. Waqar, K. K. Wong, K. F. Tong, A. Sharples, and Y. Zhang, "Deep learning enabled slow fluid antenna multiple access," *IEEE Commun. Letters*, vol. 27, no. 3, pp. 861–865, Mar. 2023.

[16] A. Froytlog *et al.*, "Ultra-low power wake-up radio for 5G IoT," *IEEE Commun. Mag.*, vol. 57, no. 3, pp. 111–117, Mar. 2019.

[17] K. K. Wong, K. F. Tong, Y. Chen and Y. Zhang, "Closed-form expressions for spatial correlation parameters for performance analysis of fluid antenna systems," *IET Elect. Letters*, vol. 58, no. 11, pp. 454–457, May 2022.

[18] T. S. Rappaport, G. R. MacCartney, M. K. Samimi, and S. Sun, "Wideband millimeter-wave propagation measurements and channel models for future wireless communication system design," *IEEE Trans. Commun.*, vol. 63, no. 9, pp. 3029–3056, Sept. 2015.

[19] J. Fiorina and W. Hachem, "On the asymptotic distribution of the correlation receiver output for time-hopped UWB signals," *IEEE Trans. Sig. Process.*, vol. 54, pp. 2529–2545, Jul. 2006.

[20] M. Abramowitz and I. A. Stegun, *Handbook of Mathematical Functions with Formulas, Graphs, and Mathematical Tables*, Dover Publications Inc.; New edition, Sixth Printing, Nov. 1967, with correlations.